EFFECT OF DILATANCY ANGLE ON BEARING CAPACITY OF FOOTING

Umashankar B., Assistant Professor, Indian Institute of Technology Hyderabad, India, buma@iith.ac.in
Rajashekhar M., Masters' Student, Indian Institute of Technology Hyderabad, India, ce13m0001@iith.ac.in

ABSTRACT: In Mohr-Coulomb failure criterion, the angle of shearing resistance of soil ϕ is assumed to be constant along the slip plane. However, over the second half of the last century, it is well recognized that the dilatancy angle influences the shear strength of sand. Many researchers have proposed correlations between the angle of shearing resistance at peak state in terms of intrinsic soil variables and soil state variables. Studies on the effect of dilatancy angle of soil, ψ, on the load-settlement response of a strip footing are available in the literature. However, in most of these studies, ψ equal to zero or equal to angle of shearing resistance of soil, ϕ, is assumed, and only limited studies are available to predict the load-settlement response of strip footing when the dilatancy angle of sand lies between zero and ϕ. In the present study, the effect of dilatancy angle of sand on the load-settlement response of a rigid strip footing resting on sand and on the formation of slip planes is studied by varying the dilatancy angle ranging from zero to the angle of shearing resistance of soil (*i.e.*, ψ =0 to ϕ).

INTRODUCTION

The simple frictional model for the failure of soil based on Coulomb's pioneering work in 1773 is familiar to all geotechnical engineers and is conventionally shown on the Mohr's circle diagram (Fig. 1). The frictional relationship is expressed in terms of effective stresses. If the vertical movements and the shear displacements are measured in simple test, then a dense sand usually dilates, that is, it expands in volume as the sample continues to shear. The dilation takes place after small initial compression. The magnitude of dilation mainly depends on the density of soil. As the density increases, the magnitude of dilation increases.
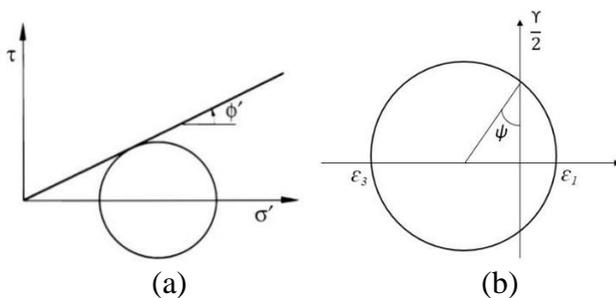

Fig. 1 Mohr's circle showing, (a) shear strength failure criterion, and (b) strain rate

In simple terms, the angle of dilation is defined as the change in volume to the unit change in shear strain. But extending the definition of dilatancy angle definition of angle of dilation for other than plane strain conditions needs to be treated with more care. The usual definition can be expressed in the following is

$$sin(\Psi) = \frac{-(\varepsilon_1 + \varepsilon_2 + \varepsilon_3)}{(\varepsilon_1 - \varepsilon_3)} \qquad (1)$$

where, $\varepsilon_1, \varepsilon_2, \varepsilon_3$ = strains in x, y, z directions.

The minus sign is due to the sign convention that compressive stresses and strains are taken as positive in soil mechanics, so that the angle of dilation is positive when soil expands.

$$sin(\Psi) = \frac{-(\varepsilon^p_1 + \varepsilon^p_3)}{(\varepsilon^p_1 - \varepsilon^p_3)} \qquad (2)$$

where, $\varepsilon^p_1, \varepsilon^p_3$ = plastic strains in 1 and 3 (or x and z) directions.

For the plane-strain condition (ε_2=0), Eq. 1 reduces to Eq. 2. Other major distinction is that dilatancy angle should be strictly defined in terms of plastic components of strain rates, but not the total strain rates. The strain rates can be divided into elastic (recoverable) and plastic (irrecoverable).
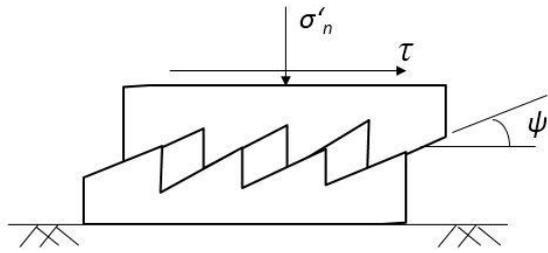
Fig. 2 The saw tooth model for dilatancy (modified after Houlsby, 1991 [3])

In order to understand the concept of dilatancy angle, physical analogy of the saw tooth model is used, as shown in Fig. 2. From this it can be observed that the dilatancy angle equals to the instantaneous angle of motion of sliding blocks relative to the rupture surface.

LITERATURE REVIEW

Dilatancy angle is an important parameter as it accounts for the appropriate friction angle in analyzing any problem. In the present study, significance of dilatancy angle of soil is illustrated through common geotechnical problems. Three such problems available in the literature (Houlsby, 1991 [3]) are highlighted:

1) A slope in which, the soil is free to move as relatively unconfined condition is practical ,
2) A surface footing in which the soil is free to move in a relatively unconfined manner,
3) A flexible tunnel lining in which the level of confinement is increased,
4) An axial pile loading in which the soil in the vicinity of pile is highly constrained.

Slope stability analysis was carried out by Zienciewicz et al. 1975 [10], using finite element method with frictional angle of 20^0: one with dilatancy angle equal to zero and in another with dilatancy angle equal to frictional angle (i.e., 20^0). The displacement vectors plot for the slope is shown in Fig. 3.

The problem of bearing capacity of footing was studied numerically by Zienciewicz et al. 1975 [10]. The effect of dilation was analyzed in two studies, in one case the angle of dilation is 20^0 and in another angle of dilation is 40^0. Fig. 4 (a) shows the load-settlement response of circular footing

with settlement factor on X-axis and load factor i.e. a ratio of load to cohesion of soil on Y-axis.
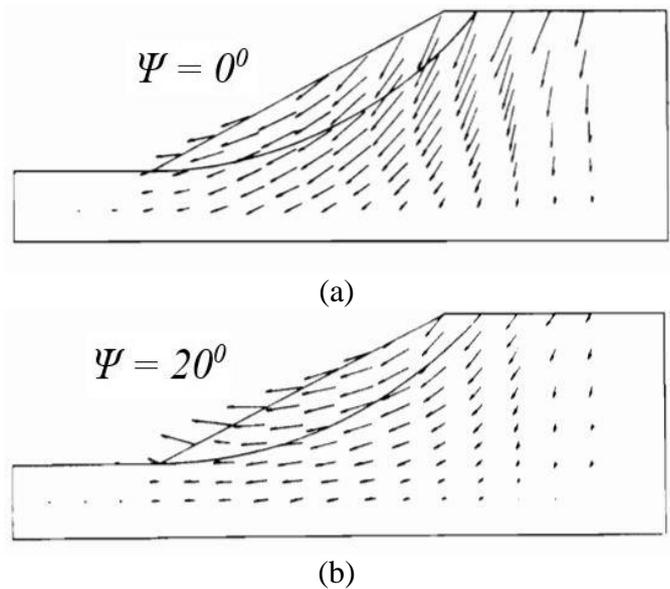

(a)

(b)

Fig. 3 Displacement vectors of soil slope (a) $\psi = 0^0$, (b) $\psi = 20^0$. (After Zienciewicz et al., 1975 [10])
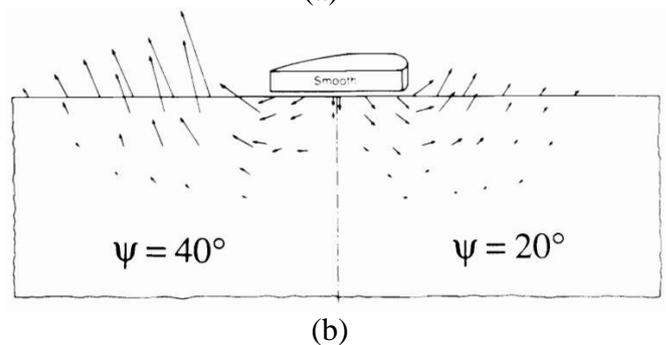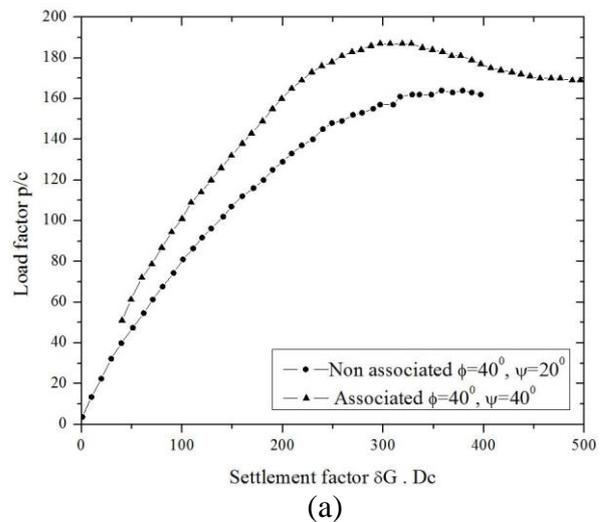

(a)

(b)

Fig. 4 (a) Load-settlement curve, (b) Displacement vectors under the foundation (After De Borst and Vermeer, 1984 [2])

Fig. 4 shows the load-deformation curves for circular footing. Analysis formed with higher angle of dilation showed a peak bearing capacity. The value was about 13% higher than that of a lower dilation angle. But at large deformations, both the cases converged to the same bearing capacity. The rate of volume change (i.e. dilation) does have a little significance on the bearing capacity of footing.

Zienciewicz et al. 1975 [10], also analyzed the problem of flexible tunnel lining. Both Pressures on a tunnel lining and ground movements around it are studied for various construction procedures. The influence of the dilation angle on the final deformations of the tunnel lining is shown in Fig. 5. Much larger movements are observed for the soil with higher dilation angle.
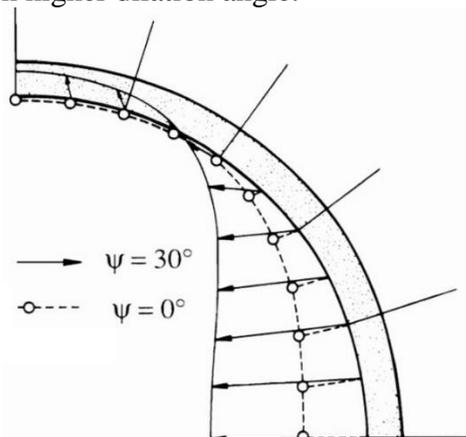

Fig. 5 Deformations of tunnel lining. (Houlsby, 1991 [3])

The conditions around a pile impose more kinematic constraint on soil movements (Fig. 6). The influence of dilatancy on both end bearing capacity and the skin friction of piles was studied. The pressures on the tip of a driven pile are estimated using spherical cavity expansion theory by Yu, 1990 [8], Yu and Houlsby, 1991 [9].

The variation of cavity expansion with different dilatancy angles are shown in Fig. 7. The cavity pressure has been divided by the isotropic stress p_0 at large distance from pile.
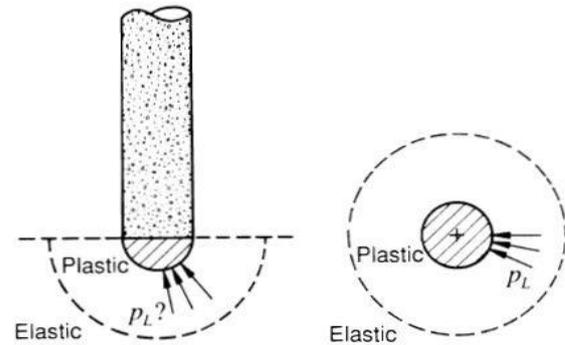

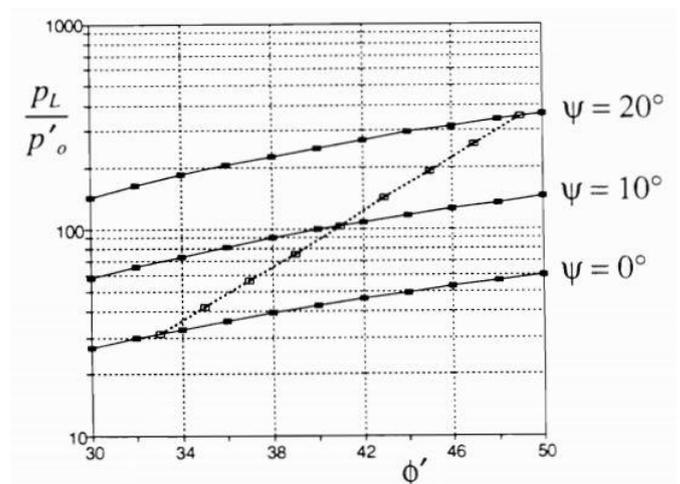**Fig. 6** Idealization of a pile end-bearing as a spherical cavity expansion (Houlsby, 1991 [3])

Fig. 7 Axial pile loading (Houlsby, 1991 [3])

The three main curves shown are the pressures calculated for dilatancy angles equal to 0^0, 10^0 and 20^0. The calculated end- bearing capacity increases more than fivefold as the dilatancy angle increases from 0^0 to 20^0. From this study, it can be stated that the influence of dilatancy angle increases with the increase in the confinement of the soil.

NUMERICAL MODELING

Validation with Potts model
For the initial validation of model, Potts, 2003 [4] was considered. Potts, 2003 [4], used finite element method to study the effect of dilatancy angle in various cases. In the present study, a smooth, rigid strip surface foundation was considered. The soil parameters used in the paper are as follows:

deformation modulus, E= 10 MPa, Poisson's ratio, $\nu = 0.3$, c = 0 kPa, $\phi = 24^0$, the initial stresses in the soil were calculated on the basis of saturated bulk unit weight = 20kN/m^3, ground water table is at the soil surface.
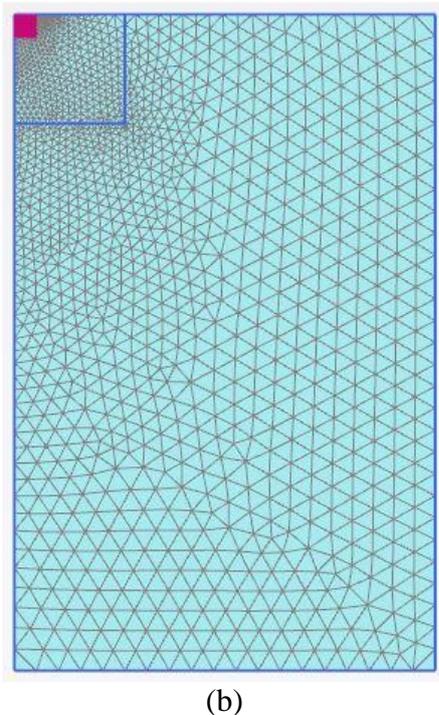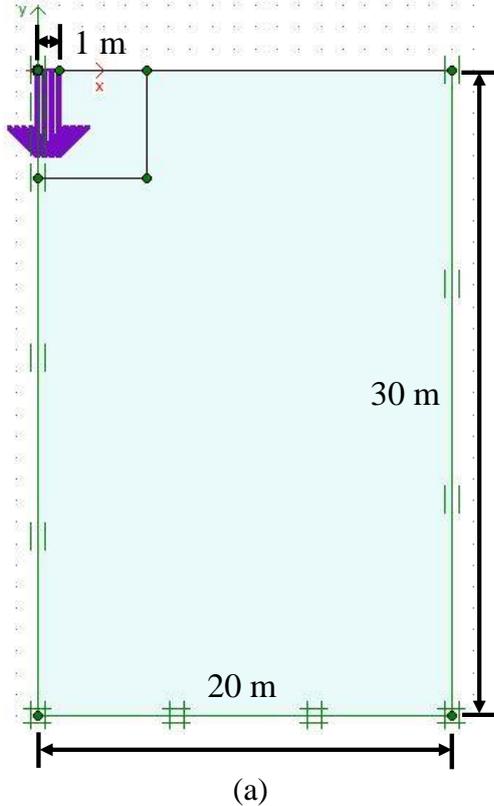

(a)

(b)

Fig. 8 PLAXIS 2-D Model showing (a) geometry, and (b) mesh generation

A finite element software PLAXIS-2D version 2012 was used to model the problem. Mohr-Coulomb failure criterion was used to represent the soil material. Table 1 gives the soil properties considered in the study. A fine mesh with average element size of 0.444 m was used and the total number elements in the model were equal to 2892. Figs. 8(a) and 8(b) show the model used in PLAXIS-2D software and the mesh generation in process of analysis. The boundary distances are determined by performing boundary effect analysis such that the boundary distance has no effect on the results. The depth of the model was taken as 30 times the width of the footing. While the boundaries on the left and right were taken as 20 times the width of the footing from the axis of symmetry. The lateral boundaries of the model were fixed in the horizontal direction, and bottom of the model was fixed in both the directions. Clustered mesh technique was adopted during mesh generation. In this technique, the mesh near the area of the interest can be densified. From Fig. 8(b), it can be observed that mesh is dense (fine refinement) near the loading area and gets less dense (coarse refinement) as the distance from the load increases.

Table 1 Material Properties of soil

Material Property	Value
Deformation Modulus (MPa)	10
Cohesion (kPa)	1
Poisson's ratio	0.3
Prescribed displacement (mm)	25
Unit weight (kN/m^3)	20
Angle of shearing resistance(ϕ)	24^0
Dilatancy angle (ψ)	$0^0 - 24^0$

Model considered in the present study was validated against Potts model. The results from the present study and Potts model are presented in Fig. 10. The results from the present study were found to be in good agreement with the Potts model and the percentage difference between these two analyses was only about 2.4%.
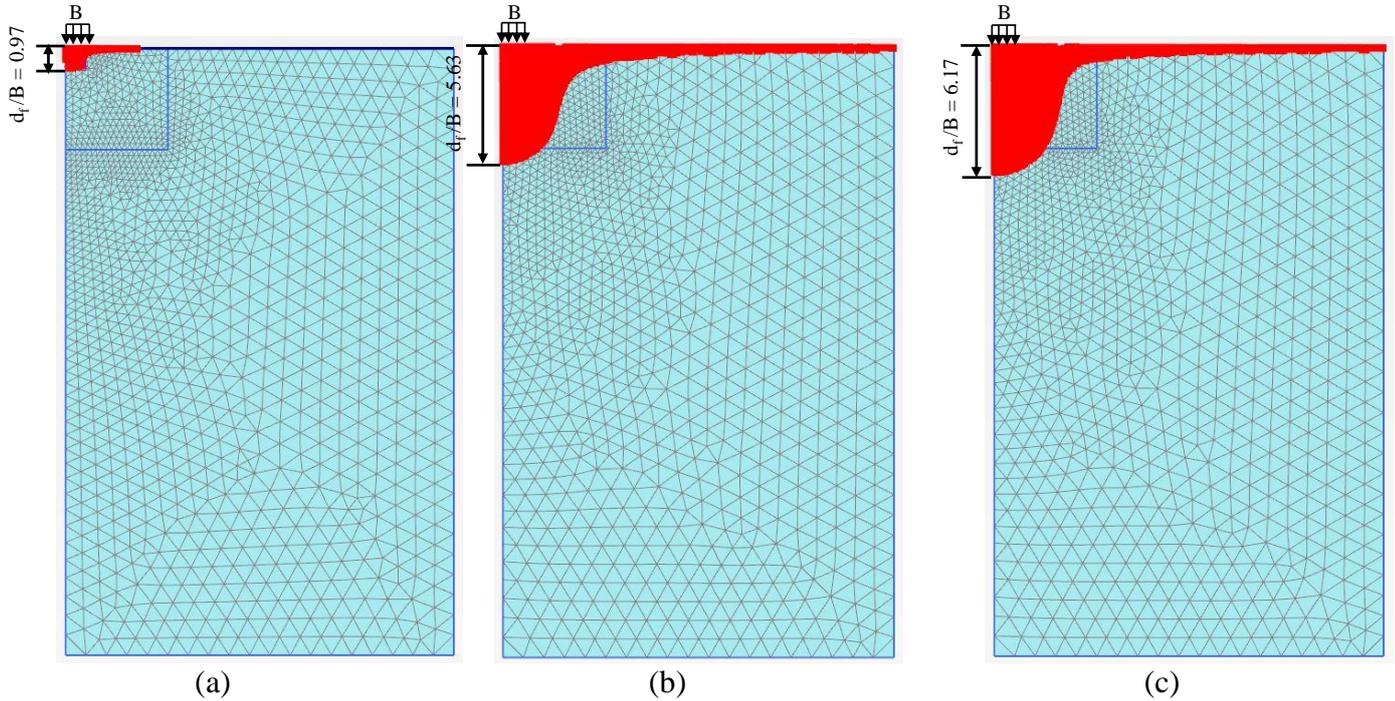
(a)   (b)   (c)

Fig. 9 Plastic zone formation in cases (a) $\psi=0^0$, (a) $\psi=10^0$, (c) $\psi=24^0$ and $\phi=24^0$
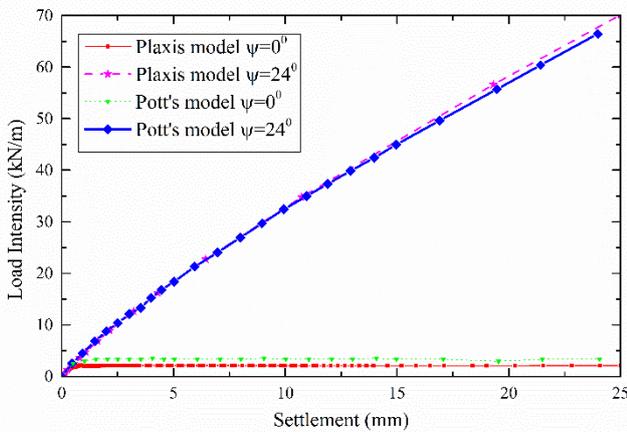

Fig. 10 Validation of load-Settlement response from present study and Potts model

Variation of load-settlement curve of soil

Potts, 2003 [4] have studied the extreme cases only (i.e., $\psi=\phi=24^0$). In this study, the effect of dilatancy angle on bearing capacity with various dilation angles between 0^0 and ϕ was studied. The same model dimensions and the materials properties given in the above section was used.

Present study was aimed to examine the behavior of load-deformation curves for various dilatancy angles and the formation of slip lines which indicates the plastic zone formation below the footing. Fig. 11 shows the load-settlement variation with the settlement of the footing for dilatancy angles ranging from zero to the angle of shearing resistance of the soil.
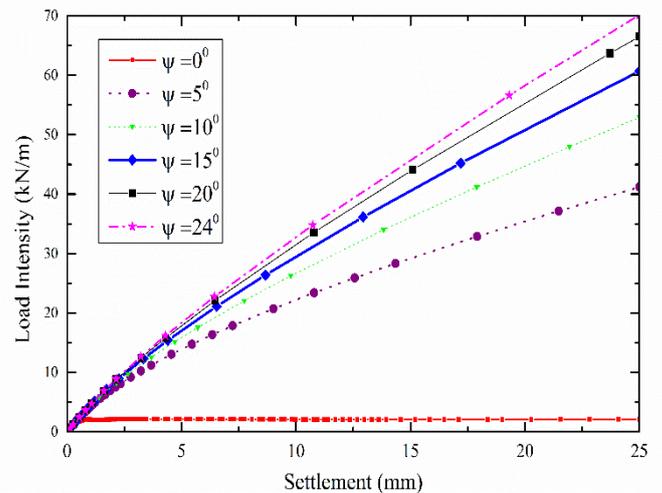

Fig. 11 Load-settlement response of footing for $0^0<\psi<24^0$

Comparison of results indicate that dilation not only affects the limit loads, but also dominates the load-settlement behavior. The higher the dilatancy angle, the stiffer the load-settlement curve. Consequently, the analysis with the angle of dilation is equal to zero ($\psi = 0^0$) is the only possible way to predicts an ultimate load. Though most of sand in the field will exhibit some amount of dilation, but predictions during design of any footing is based on $\psi=0^0$ and are likely to be very conservative.

Variation of Plastic zone formation

Fig. 9 shows the variation of plastic zone formation below the strip footing. It can be observed that as the dilation of the soil is increased, the plastic zone formation has changed drastically. The formation of plastic zone is very significant even in the case of $\psi =10^0$. An approximately 10% increase in the depth of formation failure zone is observed when the ψ is increased from 10^0 to 24^0.

CONCLUSIONS

The effect of the dilation angle of the soil on the load-settlement curve of a rigid strip load was analyzed and following conclusions are made:

- Limit load was reached within the range of settlements considered in the study only when $\psi =0^0$ was considered. For this case, the ultimate capacity can be predicted at displacement of 25mm i.e. 1.2% of width of footing.
- The depth of plastic zone formation below the footing increases by 10% with increase in angle of dilation angle from 10^0 to 24^0. The increase in the plastic zone was much higher when ψ is increased from 0^0 to 24^0.

REFERENCES

1. Bolton, M.D. (1986), The strength and dilatancy of sands, *Geotechnique,* 36(1), 65-78.
2. De Borst, R. and Vermeer, P.A. (1984) Possibilities and Limitations of Finite Elements for Limit Analysis, Geotechnique, 34(2), 199-210.
3. Houlsby, G.T. (1991), How the Dilatancy of soils affects their behaviour*, 10th Euro. Conf. on Soil Mech. and Found. Engg.*, Report number OUEL1888/91.
4. Pott's, D.M. (2003), Numerical analysis: a virtual dream or practical reality? *Geotechnique,* 53(6), 535-573.
5. Rowe, P.W. (1962), The stress – dilatancy relation for static equilibrium of an assembly of particles in contact, *Proc. R. Soc. A*, 264, 500-527.
6. Salgado, R. (2011), The Engineering of foundations, Tata McGraw-Hills Edition 2011.
7. Schanz, T. and Vermeer, P.A. (1996), Angle of friction and dilatancy of sand*, Geotechnique* 46(1), 145-151.
8. Yu, H.S. (1990), Cavity Expansion Theory and Its Application to the Analysis of Pressure meters, *D.Phil Thesis*, University of Oxford.
9. Yu, H.S. and Houlsby, G.T. (1991), Finite Cavity Expansion in Dilatant Soils: Loading Analysis, *Geotechnique,* 41(2), 173-184.
10. Zienciewicz, O.C., Humpheson, C. and Lewis R. W. (1975), Associated and Non-Associated Visco-Plasticity and Plasticity in Soil Mechanics, *Geotechnique,* 25(4), 671-689.